NASA TECHNICAL MEMORANDUM NASA TM X-1603

NASA TM X-1603

USE OF WIRE LACING TO REDUCE BLADE VIBRATION IN AN AXIAL-FLOW COMPRESSOR ROTOR

by Roy D. Hager, George W. Lewis, and Jack M. Wagner

Lewis Research Center
Cleveland, Ohio

NATIONAL AERONAUTICS AND SPACE ADMINISTRATION • WASHINGTON, D. C. • JULY 1968

NASA TM X-1603

USE OF WIRE LACING TO REDUCE BLADE VIBRATION IN AN AXIAL-FLOW COMPRESSOR ROTOR

By Roy D. Hager, George W. Lewis, and Jack M. Wagner

Lewis Research Center
Cleveland, Ohio

NATIONAL AERONAUTICS AND SPACE ADMINISTRATION

For sale by the Clearinghouse for Federal Scientific and Technical Information
Springfield, Virginia 22151 – CFSTI price $3.00

ABSTRACT

The experimental axial-flow compressor rotor had a diameter of 20 inches (50.8 cm), a hub-tip radius ratio of 0.4, and a blade aspect ratio of 3.6. The rotor was tested with lacing wires installed near the blade leading and trailing edges close to the blade tip. The wires were installed to reduce a severe bending vibration encountered at approximately 45 percent of design speed. Blade vibratory stresses were reduced from approximately ±110 000 psi ($\pm 75.902\times10^{7}$ N/m^2) for the undamped blade to approximately ±1550 psi ($\pm 1.070\times10^{7}$ N/m^2) for the blade with lacing wires. An estimated reduction in the overall rotor efficiency of 1.6 percentage points resulted from the use of the wires.

STAR Category 01

USE OF WIRE LACING TO REDUCE BLADE VIBRATION IN AN AXIAL-FLOW COMPRESSOR ROTOR

by Roy D. Hager, George W. Lewis, and Jack M. Wagner
Lewis Research Center

SUMMARY

A 20-inch- (50.8-cm-) diameter experimental axial-flow compressor rotor with a blade aspect ratio of 3.6 and a hub-tip radius ratio of 0.4 was tested with two lacing wires, one installed near the blade leading edge and the other near the blade trailing edge 0.7 inch (1.78 cm) from the blade tip. These wires served to reduce a severe blade bending vibration encountered at approximately 45 percent of design speed. The selection of wire size and material was based on a stress analysis and wear tests. The wear tests determined wire and blade wear compatibility. Wire sizes were kept to a minimum to reduce the aerodynamic losses.

The wire lacing in the rotor reduced the blade vibratory stresses from ±110 000 to ±1550 psi ($\pm 75.902\times10^{7}$ to $\pm 1.070\times10^{7}$ N/m^2) at approximately 45 percent of design speed. A maximum vibratory stress of ±2600 psi ($\pm 1.794\times10^{7}$ N/m^2) occurred at 90 percent of design speed. A map of the complete compressor performance was obtained after the lacing wires were installed. After more than 30 hours of operation, only slight burnishing of the wire was observed. The total-pressure loss associated with the lacing wires reduced the mass-averaged peak efficiency at design speed by an estimated 1.6 percentage points.

INTRODUCTION

Compressor blades are occasionally subjected to high vibratory stresses. Over a period of time, these stresses can cause blade fatigue failure. Such a failure occurred during a test of a 20-inch- (50.8-cm-) diameter experimental axial-flow compressor rotor due to a severe resonance vibration and resulted in hairline cracks in 21 of 45 blades. The damaged blades were repaired by electron-beam welding (ref. 1). To prevent a second failure, wire lacing was installed in the repaired rotor.

This report discusses the design and installation of the wire dampers and the operational experience gained from the experimental investigation of this compressor rotor. In addition, the effects of the wires on the rotor efficiency and the results of both a damping-wire stress analysis and a wire material wear test are presented.

DESIGN STUDY

The 20-inch- (50.8-cm-) diameter experimental axial-flow compressor rotor tested has a hub-tip radius ratio of 0.4, a design rotative speed of 13 190 rpm, and a design pressure ratio of 1.53. The rotor, shown in figure 1, has 45 blades with an aspect ratio

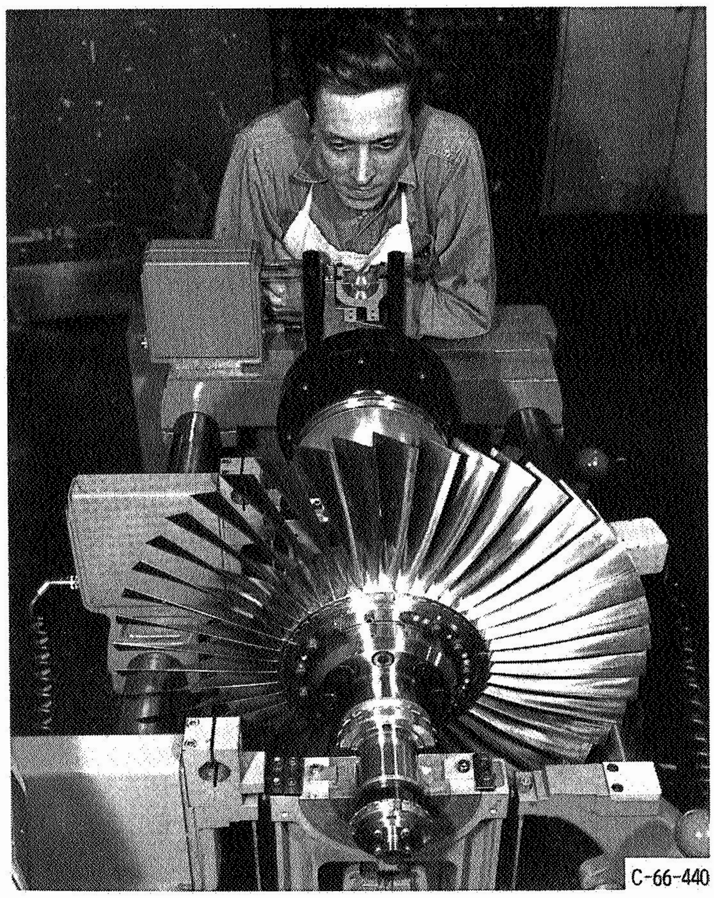

Figure 1. - Experimental axial-flow compressor rotor.

of 3.6. During the test, this rotor failed at approximately 45 percent of design speed as the result of a severe first-mode bending vibration. A blade vibratory stress of ±110 000 psi ($\pm 75.902\times10^{7}$ N/m^2) and a small torsional blade stress were observed just before failure. The design of a tandem lacing wire that served as a vibration damper and a simplified stress analysis that aided in the selection of the wire size are presented in the following sections. Also, since relative motion exists between the wire and the blade, consideration is given to the wear properties of the wire material.

General Considerations

The design of lacing wires that will reduce blade vibration requires the consideration of the mechanisms involved in damping with tandem lacing wires. Two principal mechanisms are (1) the damping of the vibration by friction between the wire and blade, and (2) the restraining of the blade through binding and wire flexure resulting from the blade motion not being parallel to the wire axis. In the mechanism of friction, as the blades have slightly different natural frequencies and will therefore be out of phase during vibration, relative motion exists between the wire and the blade. The centrifugal force between the blade and the wire creates a friction force that tends to restrict the blade motion. This force varies with the centrifugal loading on the wire and with the coefficient of friction between the wire and the blade. Wires located near the blade tip exert a large centrifugal force on the blade. One of the most common types of blade vibration is that in which the blades tend to bend about the hub so that the tip has the greatest amplitude (first-mode bending). In first-mode bending, wires located near the blade tip have a greater relative motion with respect to the blade and also a high centrifugal force on the blade. Therefore, lacing wires installed near the blade tip are the most effective in damping this mode of blade vibrations.

In the second mechanism of damping, the blade is restrained as the result of binding and flexure. The blade tip section with the tandem lacing wires installed is shown in figure 2(a). The blade bending motion, shown in figure 2(a), blade number 1, is not parallel to the damper wire axis. Thus, a restraining force is exerted on the blade as it flexes the wire sideways.

Both mechanisms of damping relate to torsional mode blade vibrations (fig. 2(a), blade number 2). As the blade twists, it binds on the wire and thus its motion is restricted. Relative motion can also exist between the wire and the blade producing friction damping. For the torsional mode, the most effective damping is achieved with two tandem lacing wires, one mounted near the blade leading edge and the other near the trailing edge. A single-wire installation can also be used for torsional damping (in addition to reducing bending vibration) if the wire is mounted near one blade edge or if the mounting hole in the blade is only slightly larger than the wire.

A kind of damping similar to mechanism (2) is shown in figure 2(b), which illustrates the wire deflection under centrifugal loading. If the wire were in this shape, any rela-

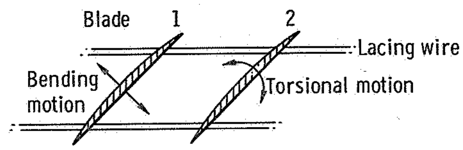

(a) View perpendicular to rotor axis.

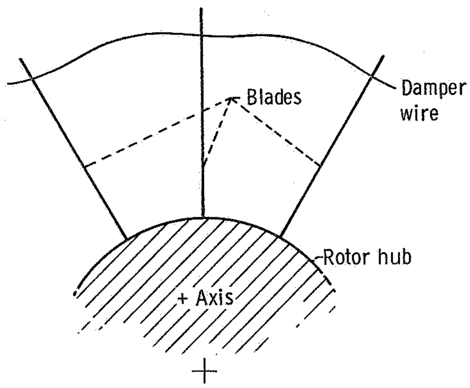

(b) View parallel to rotor axis.

Figure 2. - Typical lacing wire installation for axial-flow compressor rotor.

tive motion between the wire and the blades would cause the wire to bend. The force needed to bend the wire would restrict the blade vibration in much the same way the blade motion is restricted in torsional damping (fig. 2(a)).

During operation, the centrifugal force on the lacing wires generates both bending and tensile stresses. Since the centrifugal force increases with radius, the stress on the wire will increase with increasing radius. The determination of the wire bending stresses and tensile stresses are presented later in the report.

The wires can be expected to have a detrimental effect on the rotor aerodynamic performance: they generate wakes that cause total pressure losses which increase with the wire diameter and the flow velocity. The percentage of flow affected by the wires increases with radius; thus, the penalty on the compressor performance may be greater if the wires are located near the blade tip. The effect of wire lacing on the aerodynamic performance of a four-stage compressor equipped with lacing wires is presented in reference 2.

Apparent from the previous discussion is that the selection of wire location and size involves several compromises. For vibration damping, a large-diameter wire located near the blade tip is usually the most effective. However, in terms of wire stress, the most desirable placement of the wire is near the rotor hub. Also, with respect to aerodynamic performance, the use of a small-diameter wire located near the hubs would keep losses lower than those resulting from the use of a large-diameter wire near the blade tip.

Friction and Wear Consideration

One of the considerations in selecting a lacing wire material is the rate of wear as the wire rubs against the blade material. To aid in the selection of a wire material, wear tests were made of various wire samples as they rubbed against blocks of blade material. A typical wear test is schematically presented in figure 3. The load F represents the centrifugal force between the wire and blade. Each wire material was tested for 24 hours against a maraging steel block, the rotor blade material. The chemical composition and the mechanical properties of this blade material are listed in table I. The available wire materials were titanium and two Inconel alloys, Inconel 600 and X-750. Both Inconel alloys (tables II and III) were tested with and without an oxide coating. This coating protects the wire from wear and provides a rough surface, which gives the wire a high coefficient of friction. Two methods of oxide coating were used, in the first of which the nickel alloy wire was soaked in a salt solution to permit the formation of the nickel oxide coating. Coating the Inconel X-750 in a salt bath was difficult, and the resultant coating was patchy and uneven in thickness. In the second method, the nickel alloy was thermally oxidized. With both oxide coatings, the Inconel alloys showed negligible wear. The uncoated Inconel samples showed slightly more wear than the coated ones. During the wear tests, the oxide coating is continually replenished because the friction heat promotes oxidation. Wear visible to the eye (after the 24-hr test) was only

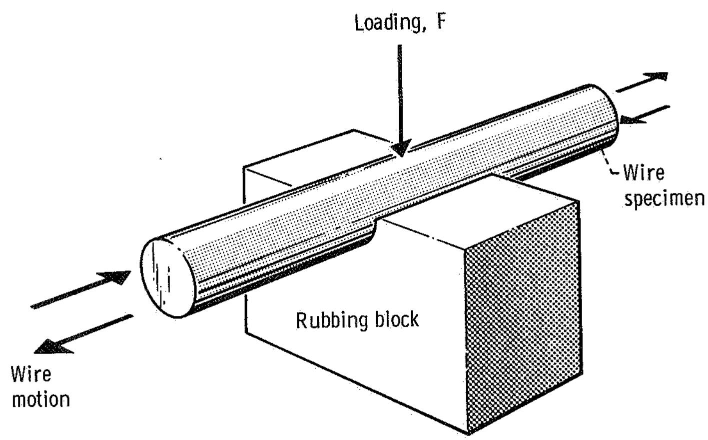

Figure 3. - Schematic diagram of wear test.

TABLE I. - PHYSICAL PROPERTIES AND CHEMICAL COMPOSITION OF MARAGING STEEL COMPRESSOR BLADE MATERIAL[a]

Composition, nominal percent:	
Iron	Balance
Carbon	0.03 (max)
Nickel	18.0
Cobalt	7.5
Molydenum	5.0
Titanium	0.20
Physical Properties:	
Density, lb/in.^{3} (kg/m^3)	0.29 (8.026×10^3)
Modulus of elasticity, psi (N/m^2)	26.5 to 27.5×10^6 (18.27 to 18.95×10^{10})
Coefficient of thermal expansion, in./in./$^\circ$F (m/m/$^\circ$C)	5.6×10^{-6} at 70 to 900 (1.01×10^{-5} at 17.8 to 482.5)
Poisson's ratio	0.26
Rockwell C hardness	44 to 48
Strength and ductility at room temperature	
0.2-percent offset yield strength, psi (N/m^2):	
Annealed[b]	95×10^3 (65.5×10^7)
Maraged[c]	200×10^3 (137.9×10^7)
Tensile strength, psi (N/m^2):	
Annealed[b]	135×10^3 (93.1×10^7)
Maraged[c]	210×10^3 (144.7×10^7)
Elongation, percent:	
Annealed[b]	17
Maraged[c]	14
Reduction of area, percent:	
Annealed[b]	75
Maraged[c]	60
Endurance limit[d], psi (N/m^2):	
Smooth bar:	
Annealed[b]	------------------
Maraged[c]	115×10^3 (79.25×10^7)
Notched bar:	
Annealed[b]	----------------
Maraged[c]	46×10^3 (31.7×10^7)

[a]Refs. 5 and 6.

[b]At 1500° F (816° C) for 1 hr; air cooled.

[c]Annealed; maraged at 900° F (483° C) for 3 hr; air cooled.

[d]Vacuum melted.

TABLE II. - PHYSICAL PROPERTIES AND CHEMICAL COMPOSITION OF INCONEL 600 WIRE MATERIAL[a]

Composition, nominal percent:	
Nickel	Balance
Carbon	0.15
Manganese	1.00
Iron	6.00 to 10.00
Sulfur	0.015
Silicon	0.5
Copper	0.5
Chromium	14.0 to 17.0
Physical properties:	
Density, lb/in.^{3} (kg/m^3)	0.304 (8.43×10^3)
Modulus of elasticity, psi (N/m^2)	31.0×10^6 (21.35×10^{10})
Poisson's ratio	0.29
Rockwell C hardness	90B to 30C
Melting range, $^{\circ}$F ($^{\circ}$C)	2500 to 2600 (1373 to 1425)
Strength at room temperature, psi (N/m^2):	
Cold drawn:	
Annealed[b]	120×10^3 (82.75×10^7)
Number 1 temperature[c]	135×10^3 (93.1×10^7)
Endurance limit[d]	52.5×10^3 (36.2×10^7)

[a]Ref. 7.

[b]At 1900° F (1038° C) for 15 min; air cooled.

[c]Work hardened.

[d]Cold drawn; stress equalized at 525° F (329° C) for 3 hr.

a slight burnishing in the contact area with a wear depth, measurable on a photomicrograph, of 0.0008 inch (2.03×10^{-3} cm).

Titanium (see table IV) was tested in an uncoated condition. The samples abraded and wore rapidly, flaking and galling in the contact area. A more detailed description of the wear test results is given in reference 3. On the basis of wear resistance, the Inconel alloys are superior to titanium.

Stress Analysis

A simplified stress calculation was made to aid in the selection of the wire material and size. The stresses are a combination of tension and bending; however, for simplicity, the tensile and bending stresses were computed separately.

As the wire deflects because of centrifugal loading, it assumes a shape similar to that shown in figure 4(a). The tensile force T is schematically shown in figures 4(a) and (b). The tensile stress S_T is computed with the assumptions that the wire takes the form of an arch and that the centrifugal force C_F is concentrated at a singel midspan point (fig. 4(b)).

TABLE III. - PHYSICAL PROPERTIES AND CHEMICAL COMPOSITION OF INCONEL X-750 WIRE MATERIAL[a]

Composition, nominal percent:	
Nickel	73.0
Carbon	0.04
Manganese	0.70
Iron	6.75
Sulfur	0.007
Silicon	0.30
Copper	0.05
Chromium	15.0
Aluminum	0.80
Titanium	2.50
Columbium	0.85
Physical properties:	
Density, lb/in.^{3} (kg/m^3)	0.298 (8.25×10^3)
Modulus of elasticity, psi (N/m^2)	31.2×10^6 (21.5×10^{10})
Poisson's ratio	0.29
Rockwell C hardness	34 to 44
Melting range, $^{\circ}$F ($^{\circ}$C)	2541 to 2600 (1395 to 1425)
Strength at room temperature, psi (N/m^2):	
As drawn	145×10^3 (99.9×10^7)
Annealed[b]	110×10^3 (75.8×10^9)
Aged[c]	204×10^3 (140.6×10^7)
Endurance limit[c]	67×10^3 (46.2×10^7)

[a]Ref. 8.

[b]At 1950° F (1065° C) for 15 min; water quenched.

[c]At 1350° F (732° C) for 16 hr; air cooled.

TABLE IV. - PHYSICAL PROPERTIES AND CHEMICAL COMPOSITION OF TITANIUM WIRE MATERIAL[a]

Composition, nominal percent:	
Titanium	90.0
Aluminum	6.0
Vanadium	4.0
Physical properties:	
Density, lb/in.^{3} (kg/m^3)	0.16 (4.43×10^3)
Modulus of elasticity, psi (N/m^2)	15.8×10^6 (10.89×10^{10})
Melting range, $^{\circ}$F ($^{\circ}$C)	2786 to 2976 (1530 to 1630)
Strength at room temperature, psi (N/m^2):	
Annealed[b]	140×10^3 (96.5×10^7)
Endurance limit[b]	75×10^3 (51.75×10^7)

[a]Ref. 9.

[b]At 1350° F (732° C) for 1 hr; furnace cooled.

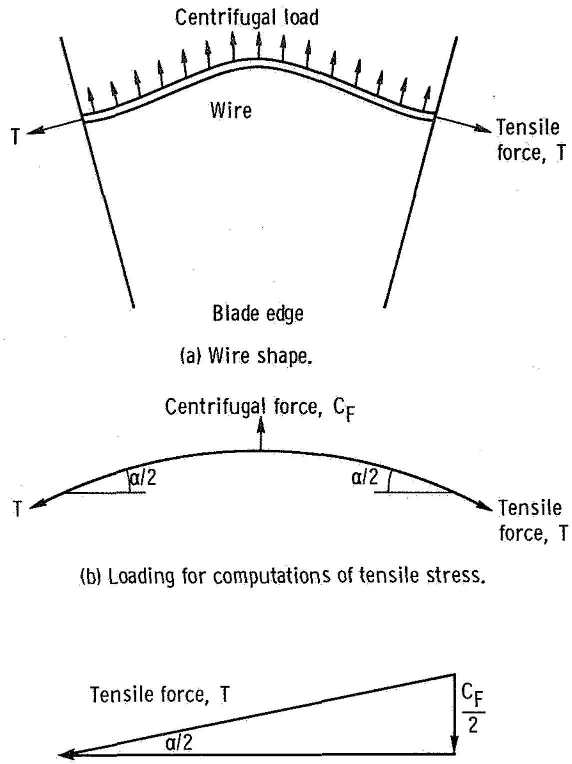

(a) Wire shape.

(b) Loading for computations of tensile stress.

(c) Summation of forces at blade edge.

Figure 4. - Assumed tensile loading in lacing wire as result of centrifugal force.

The centrifugal force C_F is defined as

$$C_F = \frac{m}{12} r\omega^2 \tag{1}$$

(All symbols are defined in the appendix.) The summation of the forces at the blade edge is shown in the vector diagram of figure 4(c), which can be used to write the equation for tensile stress

$$S_T = \frac{57.3\ C_F}{A\alpha} \tag{2}$$

For a rotor with 45 blades, α is 8^o; therefore, the computed tensile stress for the Inconel alloys is 127 000 psi (87.60×10^7 N/m^2) and 68 200 psi (47.00×10^7 N/m^2) for the titanium. The stress is constant with respect to the wire diameter.

In addition to the tensile stress, a bending stress results from the flexing of the wire under centrifugal force, with the maximum bending stresses occurring at the blade surface. Although, in the wire fibers, the bending stress is superimposed on the tensile stress, it will be computed for the case of pure bending of a simply supported beam. In reality, only a fraction of this bending stress is added to the tensile stress, since any increase in the wire tension reduces bending. Hence, the minimum wire stress is that of pure tension, and the maximum wire stress is that of pure bending. The actual wire stresses are somewhere between the two limits.

The pure-bending computations were made with the use of the assumed loading diagram shown in figure 5(a). The loading is uniformly distributed and is the result of centrifugal force exerted on the wire. Figures 5(b) and (c), respectively, indicate that maximum shear and maximum bending occur at the blades. The deflection diagram (fig. 5(d)) shows that the wire has a zero slope at the blade and a maximum deflection at midspan. The sign convention is positive for radially outward deflection.

The following equations were utilized to determine the wire stress and deflection. The equation for centrifugal force gives the load between the blade and the wire as

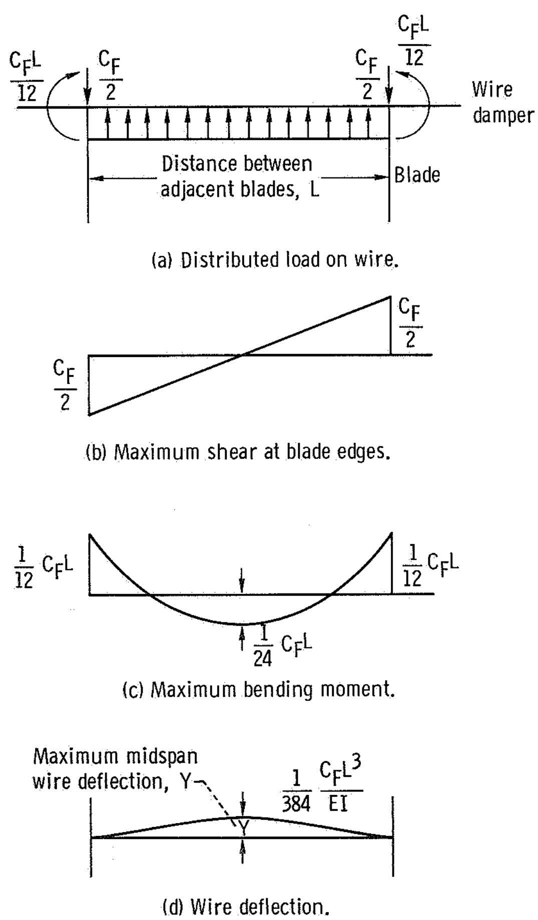

Figure 5. - Assumed beam loading for lacing wire under centrifugal load.

$$C_F = \frac{m}{12} r\omega^2 \tag{3}$$

The outer fiber bending stress is

$$S_B = \frac{Mc}{I} \tag{4}$$

The maximum bending moment is

$$M = \frac{1}{12} C_F L \tag{5}$$

Combining equations (4) and (5) gives the equation for the maximum bending stress in the wire:

$$S_B = \frac{1}{12} \frac{C_F Lc}{I} \tag{6}$$

The maximum midspan wire deflection can be expressed as

$$Y = \frac{1}{384} \frac{C_F L^3}{EI} \tag{7}$$

The centrifugal force between the wire and the blade, the maximum bending stress, and the maximum deflection as functions of the wire diameter are shown in figure 6 for Inconel and titanium wire materials. The data for these curves were computed at the design rotor speed of 13 190 rpm with the damping wire located at a radius of 9.299 inch (23.6 cm). Figure 6(a) shows that the centrifugal force between the wire and blade increases with the wire diameter and density. The maximum bending stress shown in figure 6(b) increases with decreasing wire diameter and wire densities. Figure 6(c) shows the maximum deflection due to centrifugal force and the reduction in deflection with increasing wire diameter. The deflections for titanium and Inconel are virtually the same because the higher modulus of elasticity of Inconel compensates for its higher stresses.

In addition to the steady-state stress, the lacing wire is subjected to an alternating stress resulting from the slight differences in natural frequency between the rotor blades. These blades will at times vibrate out of phase, alternately compressing and extending

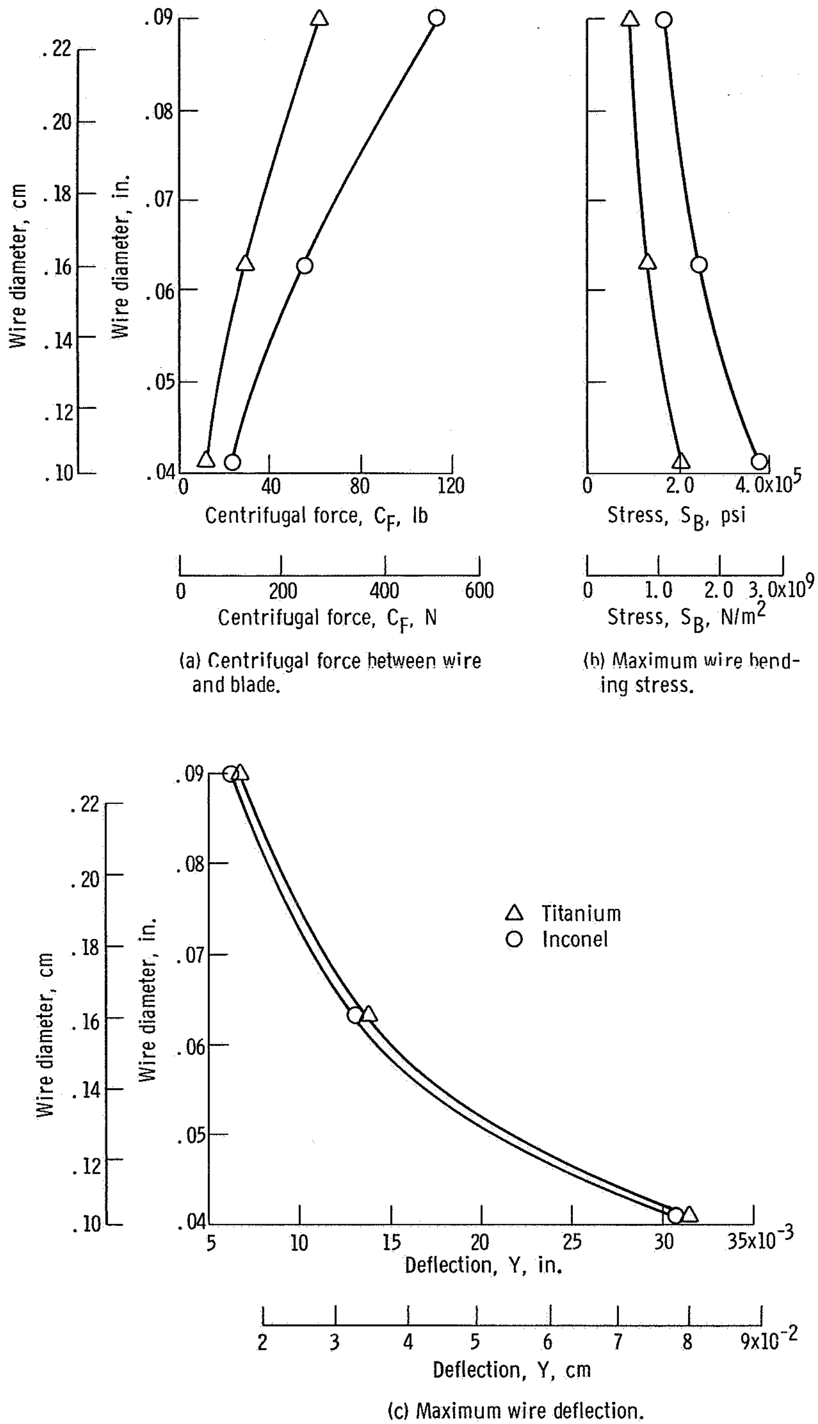

Figure 6. - Damping wire loading, stress, and deflection as function of wire diameter. Design rotor speed, 13 190 rpm; rotor radius, 9.299 inches (23.6 cm); distance between adjacent blades, 1.298 inches (3.3 cm).

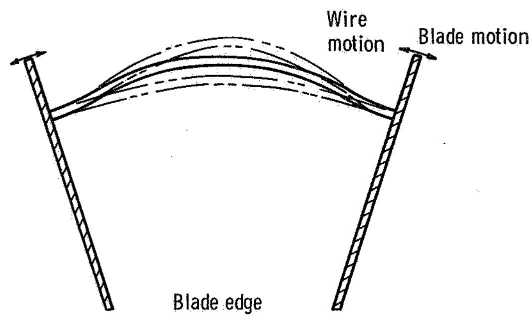

(a) Wire flexure as blades vibrate.

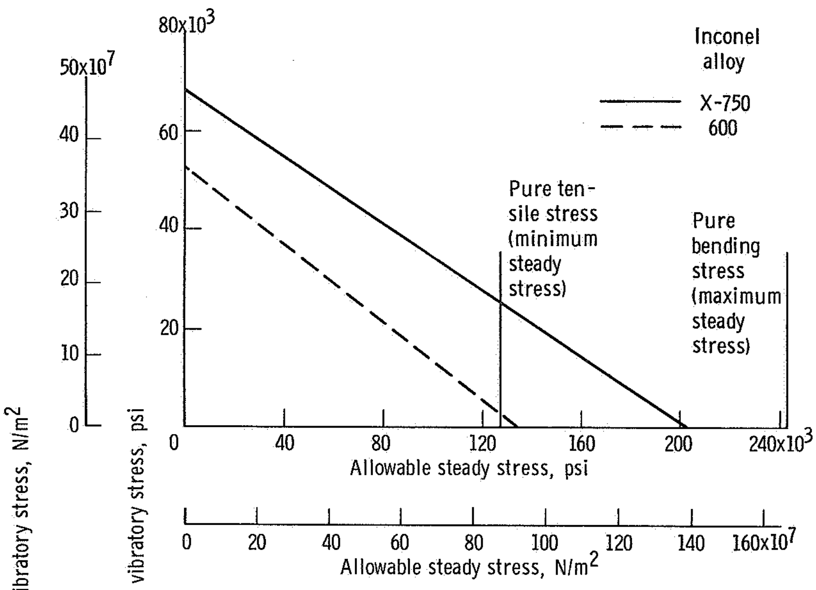

(b) Goodman diagram for Inconel alloys. Wire diameter, 0.063 inch (0.16 cm).

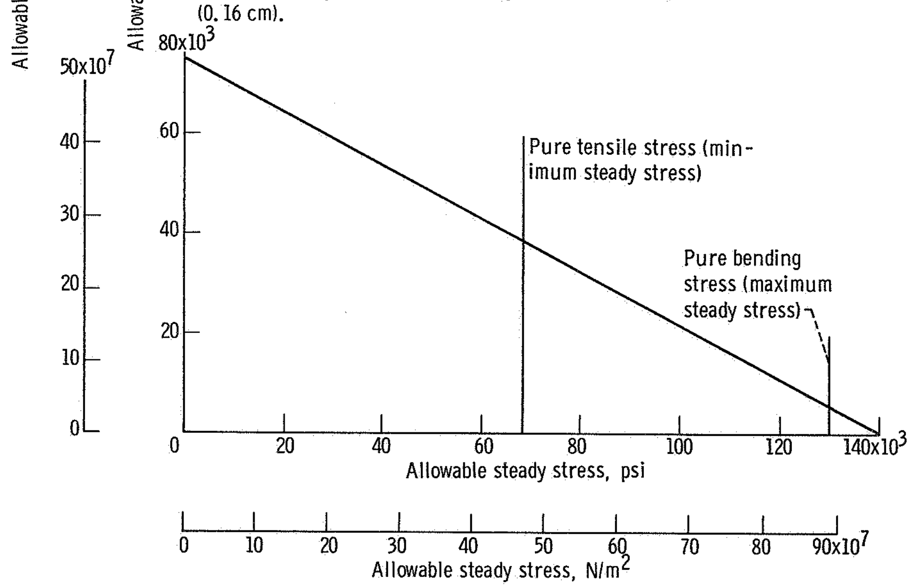

(c) Goodman diagram for titanium alloy. Wire diameter, 0.063 inch (0.16 cm).

Figure 7. - Vibratory mode of lacing wire and Goodman diagrams for three wire alloys.

the lacing wire. The wire is then loaded and unloaded, similar in manner to that of an eccentrically loaded thin column, and will flex as shown schematically in figure 7(a). The flexing produces an alternating stress that is superimposed on the steady stress. The magnitude of the stress depends on the amplitude of the blade motion and on the resulting change in shape of the wire. Since the amplitude of the blade motion cannot be predicted, the alternating stress in the wire cannot be computed. The maximum allowable wire alternating stress can, however, be obtained from a Goodman diagram if the wire steady-state stress is known.

Goodman diagrams for each of the wire materials are presented in figures 7(b) and (c). The straight line for a given wire material connects the material ultimate strength on the abscissa scale with the material endurance limit on the ordinate scale. The allowable wire alternating stress decreases as the steady stress is increased. The computed bending stress (maximum steady-state stress) and tensile stress (minimum steady-state stress) are shown in figures 7(b) and (c). The actual steady-state stress level is between the two limits. All alloys can have a steady stress above the minimum stress and still maintain an oscillating stress margin (see figs. 7(b) and (c)). However, Inconel 600 appears to be marginal whereas Inconel X-750 and the titanium alloys have an adequate stress margin.

The fact that the pure bending stress is greater than the yield stress does not necessarily mean failure if a pure bending case should occur since the outer fibers will yield to cause plastic deformation and a redistribution of the stress. A more complete explanation is given in reference 4.

Material Selection and Installation

Inconel X-750 (oxide coated) wire was chosen for lacing material because of its better wear resistance, adequate strength margin, and its ability to generate a higher centrifugal blade force. Because this alloy was unavailable at the time the rotor was reassembled, the alloy Inconel 600 was used. These two alloys have the same wear resistance. However, the allowable tensile strength of Inconel 600 is only 135 000 psi (93.2×10^7 N/m^2) as compared with 204 000 psi (140.6×10^7 N/m^2) for Inconel X-750. Inconel 600 appears to have an inadequate stress margin at 100 percent of design speed. Since stress decreases with the square of the speed, Inconel 600 would allow the rotor to be operated up to 80 percent of design speed with a stress margin similar to that which Inconel X-750 has at 100 percent of design speed. This would permit the compressor facility to be returned to operation. Two 0.063-inch- (0.16-cm-) diameter wires were installed in 0.080-inch- (0.203-cm-) diameter mounting holes located at a rotor radius of 9.299 inches (23.6 cm) or 0.7 inch (1.78 cm) from the blade tip. The axial location is 0.3 inch (0.76 cm) from the blade leading and trailing edges. Figures 8(a) and (b) show the test rotor with tandem lacing wire dampers installed. Each single lacing wire is segmented into three sections, each of which covers a circular arc of 120° or 15 of the 45 blades. The gaps between the ends of the leading edge wires are staggered with respect to the gaps of the trailing edge wires so that there is only one gap in any flow passage. The staggered gaps are shown in figures 8(a) and (b). As shown in the figure, the wire ends almost touch, forming very small gaps. These ends were later clipped close to the blades to eliminate high bending stresses in the wire as a result of the cantilevered wire ends.

The blade stresses are sensed by strain gages mounted near the blade base. Stress signals are transmitted through a slip-ring assembly and displayed on equipment in the control room. The blades are monitored concurrently.

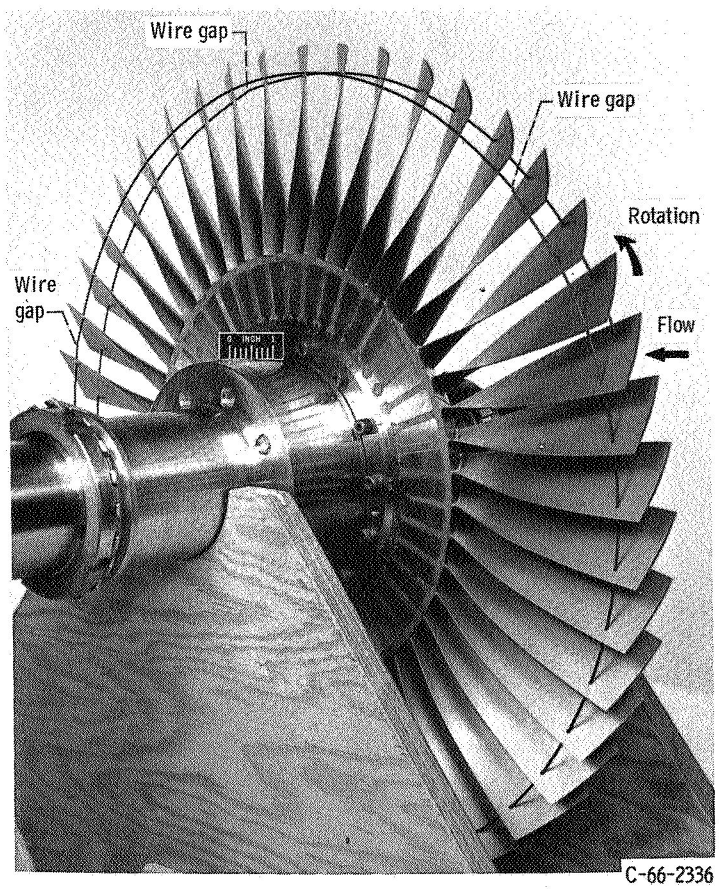

(a) Upstream view.

Figure 8. - Axial-flow compressor rotor with tandem lacing wires.

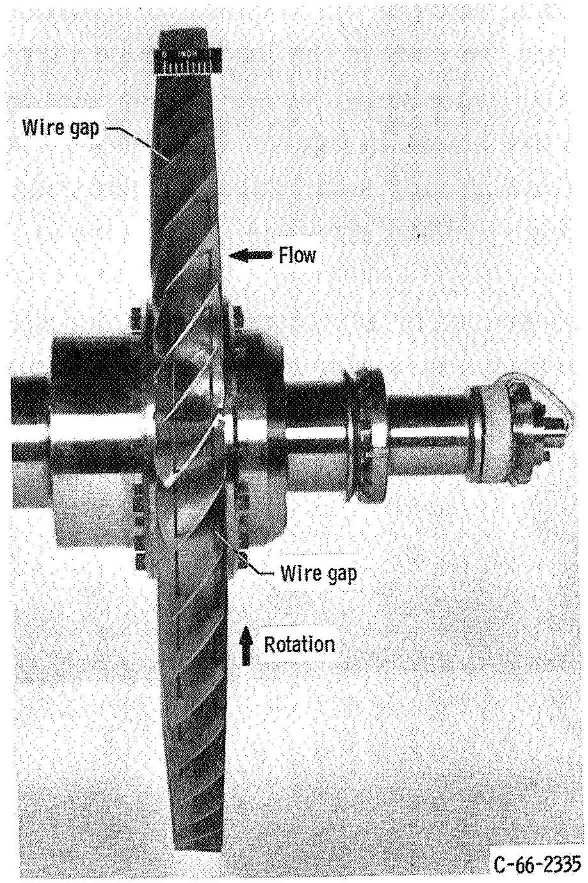

(b) Side view.

Figure 8. - Concluded.

TEST RESULTS AND DISCUSSION

Low-Speed Operation

The damped compressor rotor was run through the speed range from 0 to 50 percent of design speed (failure of the undamped blade occurred at approximately 45 percent of design speed). At 50 percent of design speed, aerodynamic testing of the rotor began. The compressor speed was increased in 10-percent increments and was inspected after each constant speed test. As the speed was increased from 80 to 90 percent of design speed, a slight increase in vibration was noted. The compressor was shut down for visual inspection, which revealed that one wire had failed at midspan between the blades. The wire also yielded near the end gaps and bent outward. This failure is shown in figure 9. A radial view into the rotor shows the wire failure (fig. 9(a)). In figures 9(b)

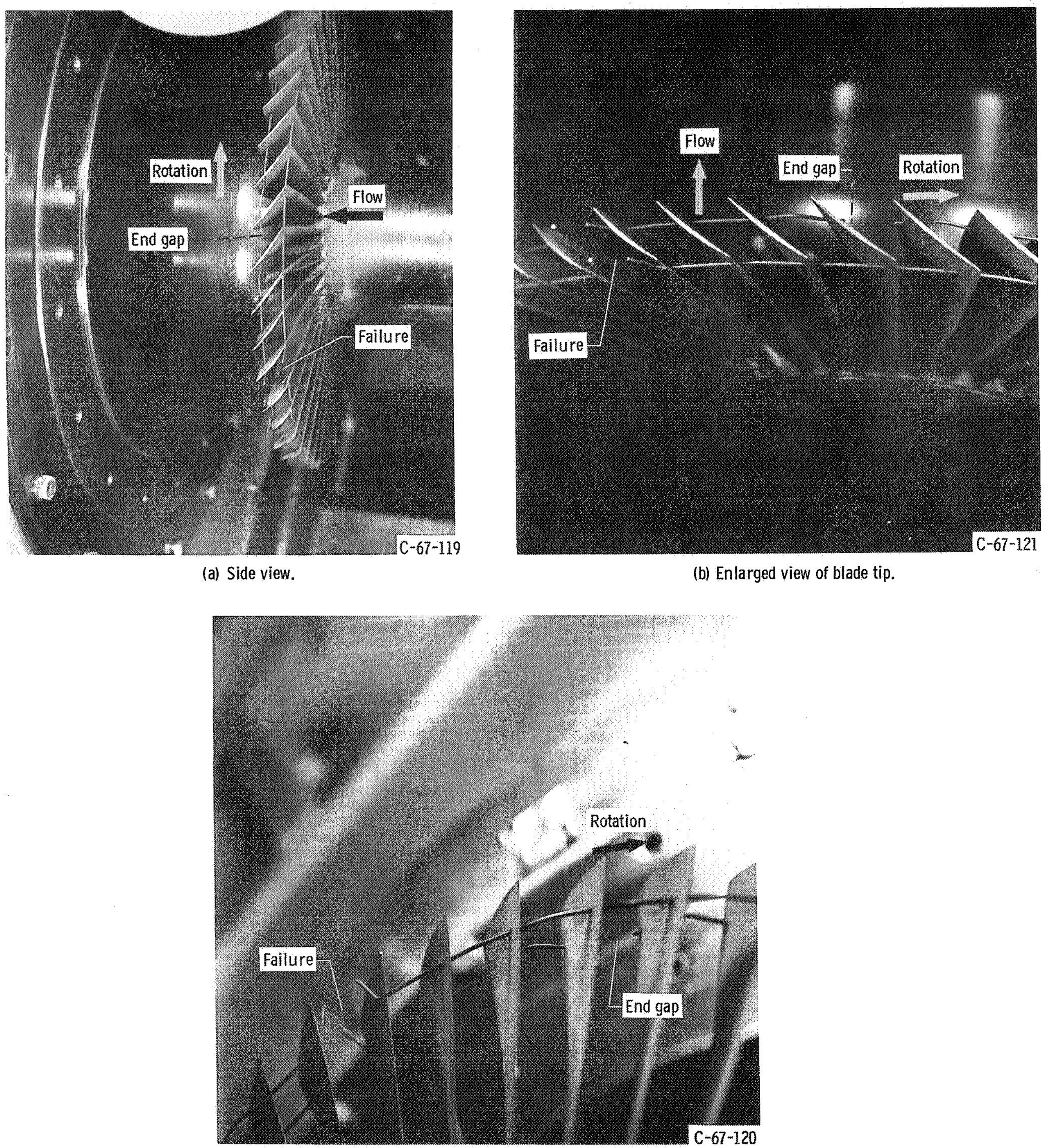

(a) Side view.

(b) Enlarged view of blade tip.

(c) Enlarged view of blade side.

Figure 9. - Axial-flow compressor rotor showing ruptured lacing wire.

and (c), the enlarged views show that the wire had broken at midspan between the adjacent blades. Other wire spans that have yielded are also visible. The wire gaps in figure 9(b) show the wire ends that were clipped to prevent cantilevering.

The Inconel 600 wire significantly reduced the vibratory stress at 45 percent of design speed, at which point the severe resonant condition caused failure of the undamped blades. This wire permitted compressor operation beyond 80 percent of design speed. The Inconel 600 wire apparently failed as a result of the combined steady and vibratory stresses. Prior to wire failure, the compressor rotor operated more than 15 hours with no sign of wire or blade wear.

High-Speed Operation

The X-750 Inconel alloy tandem wire lacing was installed in the rotor preparatory to high-speed (100 percent of design) operation. A plot of maximum measured blade vibratory stress against compressor speed is presented in figure 10 for the damped and

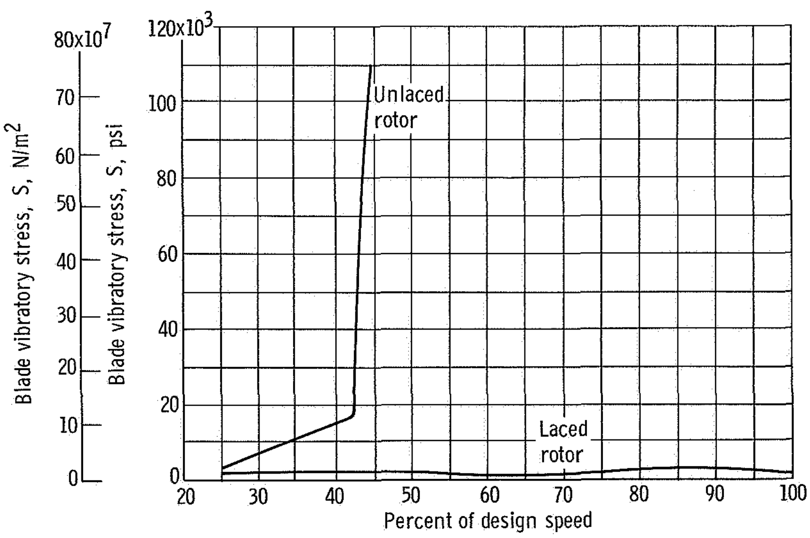

Figure 10. - Maximum measured blade vibratory stress as function of compressor speed for damped and undamped rotor. Rotor diameter, 20 inches (50.8 cm); design speed, 13 190 rpm.

undamped rotor. This figure shows the magnitude of the decrease in blade stresses from ±110 000 psi ($\pm 75.902\times10^7$ N/m^2) at approximately 45 percent design of speed to ±1550 psi ($\pm 1.068\times10^7$ N/m^2). The highest blade vibratory stress, ±2600 psi ($\pm 1.794\times10^7$ N/m^2), occurred at 90 percent of design speed. Also, the slight torsional vibration noted in the unwired rotor was considerably reduced. This vibration reduction allowed the rotor to be operated over its entire flow and speed range between 50 and 100 percent of design speed. More than 30 hours of operation were logged for the rotor equipped with lacing wire. The Inconel X-750 wires exhibited no measurable wear, only a slight burnishing at each blade contact point.

Aerodynamic Effects

At the design rotative speed, the compressor rotor equipped with tandem lacing wire exhibited an experimental peak mass-averaged temperature-rise efficiency of 88.2 percent. The spanwise variation in blade-element efficiency is shown in figure 11 as a function of radius. The radius at which the tandem lacing wire is located is also indicated. The small dot at the wire radius represents the wire size in relation to the radius scale. A decrement in efficiency exists in the region of the lacing wire and is attributed to the losses associated with the wire wake, the interference of the wire with the boundary layer growth, and the diffusion of the flow along the blade surface. It is interesting to note that, even though the wire diameter is only 0.063 inch (0.16 cm), the wire affects the efficiency profile over about 1.2 inch (3.05 cm) or 20 percent of the blade height. Fairing the curve across the efficiency profile and recomputing a mass-averaged efficiency indicates that the decrement in efficiency associated with the wires results in a

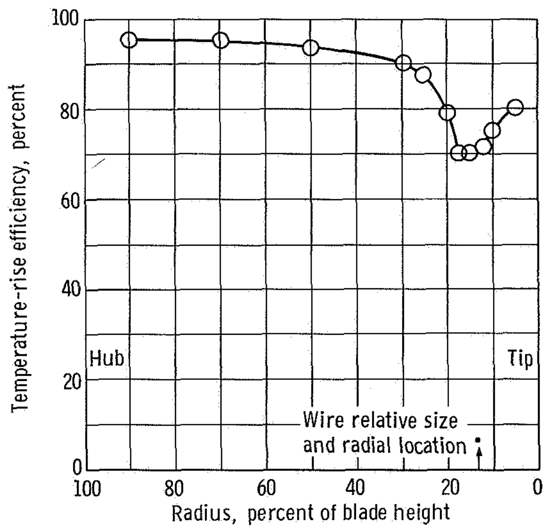

Figure 11. - Profile of axial-flow-compressor rotor efficiency as function of radius at 100 percent of design speed (13 190 rpm) for peak efficiency point.

decrease of approximately 1.6 percentage points in the overall rotor mass-averaged efficiency.

SUMMARY OF RESULTS

The following results were obtained from tests of an experimental compressor rotor on which tandem lacing wires were installed to control a severe blade bending vibration:

1. The blade vibratory stress was reduced from ±110 000 psi ($\pm 75.902\times10^{7}$ N/m^2) to ±1550 psi ($\pm 1.070\times10^{7}$ N/m^2) at 45 percent of design speed. The maximum vibratory stress at 90 percent of design speed was ±2600 psi ($\pm 1.794\times10^{7}$ N/m^2). Thus, the wires made it possible to operate the compressor rotor over its full range of flow and speed from 50 to 100 percent of design speed.

2. The compressor rotor equipped with the alloy Inconel X-750 tandem-laced damper wires was operated for more than 30 hours with no measurable wire wear, except for a slight burnishing visible at the wire contact point.

3. At design rotative speed, the compressor rotor equipped with tandem lacing wires exhibited an experimental peak mass-average temperature-rise efficiency of 88.2 percent. The decrement in the mass-averaged rotor efficiency attributed to the losses associated with the wire dampers was calculated to be 1.6 percentage points.

CONCLUDING REMARKS

The tandem-laced wire blade dampers were effective in reducing vibratory blade stresses in the 20-inch- (50.8-cm-) diameter compressor rotor. The negligible wear rate would indicate a much longer potential life than that actually logged during this test if an adequate fatigue stress margin were provided for in the wire design. This wear rate indicates that wire lacing could be used in commercial rotors where many hours of operation are required. Lacing wire dampers are, in general, cheaper and easier to install than the conventional damper shroud. Thus, wire dampers are attractive for use in research compressors where a repair might be needed to obtain performance data during a short test.

Lewis Research Center,
National Aeronautics and Space Administration,
Cleveland, Ohio, February 20, 1968,
720-03-01-48-22.

APPENDIX - SYMBOLS

A area, in.^{2}; m^2

C_F centrifugal force, lb; N

c distance to outer fiber, half wire diameter, in.; m

E modulus of elasticity, lb/in.^{2}; N/m^2

I moment of inertia of material cross-section, in.^{4}; m^4

L distance between adjacent blades, in.; m

M bending moment, (in.)(lb); (m)(N)

m mass, slugs; kg

r radius, in.; cm

S stress, lb/in.^{2}; N/m^2

T tensile force, lb; N

Y maximum midspan wire deflection, in.; m

α angle between adjacent blades, deg

ω angular velocity, rad/sec

Subscripts:

b bending

t tension

REFERENCES

1. Hager, Roy D.: Test of a Cracked Compressor Blade Repaired by Electron Beam Welding. NASA TM X-1341, 1967.

2. Andrews, S. J.; and Ogden, H.: The Effect of Lacing Wire on Axial Compressor Stage Performance at Low Speeds. Rep. No. CP-225, Aeronautical Research Counsil, Great Britain, 1956.

3. Swikert, Max A.; and Johnson, Robert L.: Friction and Wear Under Fretting Conditions of Materials for Use as Wire Friction Dampers of Compressor Blade Vibration. NASA TN D-4630, 1968.

4. Peery, David J.: Aircraft Structures. McGraw-Hill Book Co., Inc., 1950, pp. 321-322.

5. Anon.: New Breed: The Maraging Steels. Welding Des. Fabrication, vol. 39, no. 1, Jan. 1966, pp. 35-37.

6. Anon.: Maraging Steels-Processing and Fabrication. Welding Des. Fabrication, vol. 39, no. 1, Jan. 1966, pp. 37-38.

7. Anon.: Engineering Properties of Inconel Alloy 600. Tech. Bull. T-7 Table 1, Table 2 and Table 12, International Nickel Company Inc., Copyright 1962, rev. 1964.

8. Anon.: Engineering Properties of Inconel Alloy X-750. Tech. Bull. T-38 pp. 1-2, 25, and 31, International Nickel Company Inc., Copyright 1962, rev. 1964.

9. Anon.: Crucible C-120 AV Titanium Base Alloy: Data Sheet. Crucible Steel Company of America, Issue date Sept. 1, 1956, rev. May 1958, pp. 1-8.

NASA-Langley, 1968 —— 32 E-4146

NATIONAL AERONAUTICS AND SPACE ADMINISTRATION
WASHINGTON, D. C. 20546

OFFICIAL BUSINESS

FIRST CLASS MAIL

POSTAGE AND FEES PAID
NATIONAL AERONAUTICS AN
SPACE ADMINISTRATION

POSTMASTER: If Undeliverable (Section 15
Postal Manual) Do Not Retu

"The aeronautical and space activities of the United States shall be conducted so as to contribute . . . to the expansion of human knowledge of phenomena in the atmosphere and space. The Administration shall provide for the widest practicable and appropriate dissemination of information concerning its activities and the results thereof."

—NATIONAL AERONAUTICS AND SPACE ACT OF 1958

NASA SCIENTIFIC AND TECHNICAL PUBLICATIONS

TECHNICAL REPORTS: Scientific and technical information considered important, complete, and a lasting contribution to existing knowledge.

TECHNICAL NOTES: Information less broad in scope but nevertheless of importance as a contribution to existing knowledge.

TECHNICAL MEMORANDUMS: Information receiving limited distribution because of preliminary data, security classification, or other reasons.

CONTRACTOR REPORTS: Scientific and technical information generated under a NASA contract or grant and considered an important contribution to existing knowledge.

TECHNICAL TRANSLATIONS: Information published in a foreign language considered to merit NASA distribution in English.

SPECIAL PUBLICATIONS: Information derived from or of value to NASA activities. Publications include conference proceedings, monographs, data compilations, handbooks, sourcebooks, and special bibliographies.

TECHNOLOGY UTILIZATION PUBLICATIONS: Information on technology used by NASA that may be of particular interest in commercial and other non-aerospace applications. Publications include Tech Briefs, Technology Utilization Reports and Notes, and Technology Surveys.

Details on the availability of these publications may be obtained from:

SCIENTIFIC AND TECHNICAL INFORMATION DIVISION

NATIONAL AERONAUTICS AND SPACE ADMINISTRATION

Washington, D.C. 20546